Electronic Supplementary Information (ESI)

Neutral mononuclear indium(III) photosensitizers for CO_2 photoreduction

Zaichao Zhang,*[a] Li-Zhi Fu,[b] Piao He,[b] Xiao-Yi Yi*[b]

[a] *Jiangsu Key Laboratory for the Chemistry of Low-Dimensional Materials, School of Chemistry and Chemical Engineering, Huaiyin Normal University, Huai'an, Jiangsu, 223300, China*

[b] *College of Chemistry and Chemical Engineering, Central South University, Changsha, Hunan 410083, China.*

E-mail: zhangzc@hytc.edu.cn; xyyi@csu.edu.cn.

Contents

1. General Conidiations

1.1 Materials

All syntheses were carried using a standard vacuum line and Schlenk technology with an atmosphere of purified argon. Solvents for air- and moisture-sensitive manipulations were dried and deoxygenated using a JC-Meyer Phoenix solvent drying system. 2,6-di(1H-pyrrol-2-yl)pyridine[1] and substituted dipyridylpyrrole[2] were prepared according to literature methods. All other chemicals were obtained from J&K Scientific Ltd. and used without further purification.

1.2 Characterization

The ^{1}H NMR spectra were recorded on a Bruker AVANCE (III) 400M spectrometer. The infrared spectra (in KBr) were recorded on a Nicolet 6700 spectrometer FT-IR spectrophotometer. The UV-Vis spectra were recorded on an Agilent Technologies Cary 8454 UV-Vis spectrometer at ambient temperature with a 1 cm quartz cell. ESI-MS was performed on a Bruker Daltonik GmbH, Bremen mass spectrometer equipped with an electrospray ionization (ESI) source. Emission spectra were recorded on a F97Pro Fluorescence spectrometer. The quantum yields were carried out on a fluorescence spectrometer (F-7000, Hitachi, Japan) equipped with an integrating sphere, which was also reproduced on fluorescence spectrometer (FLS 1000, Edinburgh Instruments LTD.). The excited-state lifetimes (τ) were conducted on a modular fluorescent life and steady-state fluorescence spectrometer (FLS 1000, Edinburgh Instruments LTD.). Cyclic Voltammetry was performed on a CHI Instruments CHI610A electrochemical analyzer. This workstation contains a digital simulation package as part of the software package to operate the workstation (CHI version 2.06). The working electrode was a glassy carbon electrode, the counter electrode was a Pt wire, and the reference electrode was a AgCl/Ag electrode in saturated KCl. Electrochemical measurements were performed in dichloromethane solution containing 0.1 M nBu4N·PF6 electrolyte in a one compartment cell. Gas quantifications were conducted with a Shimadzu GC-2014 gas chromatograph. The photocatalytic reaction experiments are performed by the Perfect Light PCX50C photochemistry system.

X-ray Diffraction Studies: Diffraction data was record on a Bruker CCD diffractometer with monochromatized Mo-Kα radiation (λ= 0.71073 Å). The collected frames are processed using the software SAINT. The absorption correction was processed with SADABS. The structure was solved by a direct method and refined using a full matrix least squares method on F^2 with the SHELXTL software package. Atomic positions of non-hydrogen atoms were refined with anisotropic parameters. All hydrogen atoms were introduced at their geometrical positions and refined as riding atoms.

DFT calculations: DFT calculations were performed by using the Gaussian 09 package. Geometry optimizations were performed on the ground state structures with the Becke's three-parameter B3LYP exchange-correlation functional.The all-electron

Gaussian basis sets were those developed by the Ahlrichs group. The slightly smaller polarized split-valence def2-SVP basis sets for H, C, N and triple-ζ quality basis sets def2-TZVP with one set of polarization functions for the In atom. Vibrational frequencies were calculated based on the optimized structures to confirm the absence of imaginary frequencies. MOs of complexes were calculated and visualized as well. The excited states calculations were carried out on the basis of the optimized S0 structures via time-dependent DFT (TD-DFT) at the same level. The solvation effects were also taken into account using the self-consistent reaction field (SCRF) and a universal solvation model density (SMD) with the CH_3CN solvent.

Determination of Φ for CO Production. A typical experiment employed a mixture of **CoPc** (0.1 mM), PS (0.5 mM), TEOA (0.3 M) and BIH (50 mM) in 4.0 mL CH_3CN for evaluation. The temperature was kept at 25 °C. The light source is an LED light (λ = 365 nm, light intensity = 50 mW cm^{-2}, irradiated area is 0.8 cm^2). The photon flux was determined to be 1.5 × 10^{-7} einstein s^{-1}. Under these conditions, the light entering the reaction solution was considered to be fully absorbed by PS without scattering, suggesting the evaluated Φ is a lower limit. The Φ with BIH as the two-electron reductant was determined by the equation ($\Phi = n_{CO}/n_p$) for two-electron reduction of CO_2.

2. Experimental Procedures and Spectroscopic Data

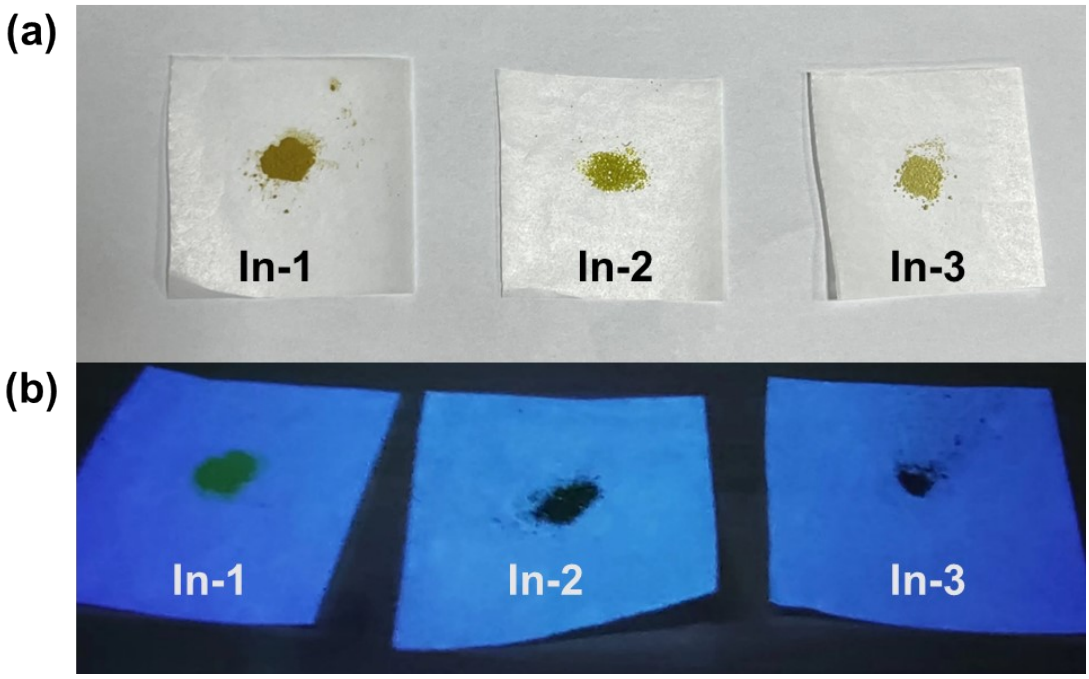

Figure S1. (a) solid samples of **In-1** – **In-3**; (b) solid samples of **In-1** – **In-3** upon irradiation at 365 nm at room temperature.

Synthesis of In-1: $InMe_3$ (24.0 mg, 0.15 mmol) was slowly added to the mixture solution of 2,5-di(pyridin-2-yl)-1H-pyrrole (110.5 mg, 0.5 mmol) and 2,6-di(1H-pyrrol-2-yl)pyridine（104.5 mg, 0.5 mmol）in toluene (5 mL). The reaction mixture was stirred for 2 hours at room temperature then heated to reflux 12 hours under nitrogen atmosphere to give a dark-green solution. After cooling, toluene was removed in vacuo. The solid residue was washed three times with diethyl ether to remove any unreacted ligand. The crude product was redissolved in CH_2Cl_2 and filtered. Recrystallized by the addition of diethyl ether to give the desired product **In-1** as a grey green solid. Yield: 100.5 mg (50%). The solution of **In-1** in CH_2Cl_2 was layered by hexane to give block single crystals which were suitable for X-ray diffraction analysis.

^{1}H NMR (400 MHz, $CDCl_3$) δ 7.79 (d, J = 5.2 Hz, 2H), 7.73 – 7.59 (m, 5H), 7.19 (d, J = 7.8 Hz, 2H), 6.92 (s, 2H), 6.86 (td, J = 5.2, 2.6 Hz, 2H), 6.80 (d, J = 3.2 Hz, 2H), 6.44 (s, 2H), 6.21 – 6.15 (m, 2H).

ESI-MS (*m/z*):543.0783, calcd. 543.0502 for [**M**]$^+$

IR (KBr, cm^{-1}): 1596 (m), 1555 (m), 1519 (m), 1431 (m), 1385 (s), 1267 (w), 1149 (w), 1031 (w), 747 (w)。

Synthesis of In-2: $InMe_3$ (34.0 mg, 0.21 mmol) was slowly added to the mixture solution of 2,6-di(1H-pyrrol-2-yl)pyridine (41.8 mg, 0.2 mmol) and 2,2'-(3,4-diphenyl-1H-pyrrole-2,5-diyl)dipyridine (74.0 mg, 0.2 mmol) in toluene (5 mL). The reaction mixture was stirred for 2 hours at room temperature then heated to reflux overnight under nitrogen atmosphere to give a dark-green solution. After cooling, toluene was removed in vacuo. The solid residue was washed three times with diethyl ether to remove any unreacted ligand. The crude product was redissolved in CH_2Cl_2 and filtered. Recrystallized by the addition of diethyl ether to give the desired product **In-2** as a yellow solid. Yield: 60 mg (43%). The solution of **In-2** in CH_2Cl_2 was layered by hexane to give block single crystals which were suitable for X-ray diffraction analysis.

^{1}H NMR (400 MHz, $CDCl_3$) δ 7.79 (ddd, J = 5.2, 1.7, 0.9 Hz, 2H), 7.72 (t, J = 7.8 Hz, 1H), 7.40 (ddd, J = 8.2, 7.4, 1.7 Hz, 2H), 7.34 – 7.30 (m, 7H), 7.29 – 7.25 (m, 4H), 7.24 (q, J = 1.2 Hz, 2H), 7.21 (s, 1H), 7.19 (s, 1H), 6.85 – 6.80 (m, 4H), 6.59 (dd, J = 2.0, 1.1 Hz, 2H), 6.25 (dd, J = 3.3, 2.0 Hz, 2H).

ESI-MS (*m/z*): 695.2136, calcd. 695.1409 for [**M**]$^+$

IR (KBr, cm^{-1}): 3426 (w), 3034 (w), 2204 (w), 1591 (s), 1553 (s), 1521 (s),1445 (s), 1321 (m), 1191 (w), 1148 (m), 1032 (m), 977 (m), 780 (m), 736 (s), 698 (m), 641 (w), 463 (w)。

Synthesis of In-3: $InMe_3$ (34.0 mg, 0.21 mmol) was slowly added to the solution of 2,6-di(1H-pyrrol-2-yl)pyridine (41.8 mg, 0.2 mmol) and 4-phenyl-2,5-di(pyridin-2-yl)-1H-pyrrole-3-carbonitrile (64.0 mg, 0.2 mmol) in toluene (5 mL). The reaction mixture was stirred for 2 hours at room temperature then heated to reflux overnight under nitrogen atmosphere to give a dark-green solution. After cooling, toluene was removed in vacuo. The solid residue was washed three times with diethyl ether to remove any unreacted ligand. The crude product was redissolved in CH_2Cl_2 and filtered. Recrystallized by the addition of diethyl ether to give the desired product **In-3** as a green solid. Yield: 75.0 mg (58%).

^1H NMR (400 MHz, $CDCl_3$) δ 8.33 (d, J = 8.1 Hz, 1H), 7.94 (d, J = 5.2 Hz, 1H), 7.89 – 7.84 (m, 2H), 7.74 (t, J = 7.8 Hz, 1H), 7.66 – 7.61 (m, 2H), 7.57 – 7.44 (m, 5H), 7.22 (t, J = 6.1 Hz, 2H), 7.12 (dd, J = 6.4, 5.3 Hz, 1H), 7.00 – 6.93 (m, 1H), 6.83 (dd, J = 3.3, 0.9 Hz, 2H), 6.47 (s, 2H), 6.22 (dd, J = 3.3, 2.0 Hz, 2H).

ESI-MS (*m/z*): 644.1718, calcd. 644.1048 for $[\mathbf{M}]^+$

IR (KBr, cm^{-1}): 3413 (w), 3060 (w), 2211 (w), 1591 (s), 1557 (s), 1518 (s), 1448 (s), 1384 (w), 1312 (w), 1152 (w), 1030 (m), 972 (w), 778 (m), 743 (m), 701 (w), 624 (w), 466 (w)。

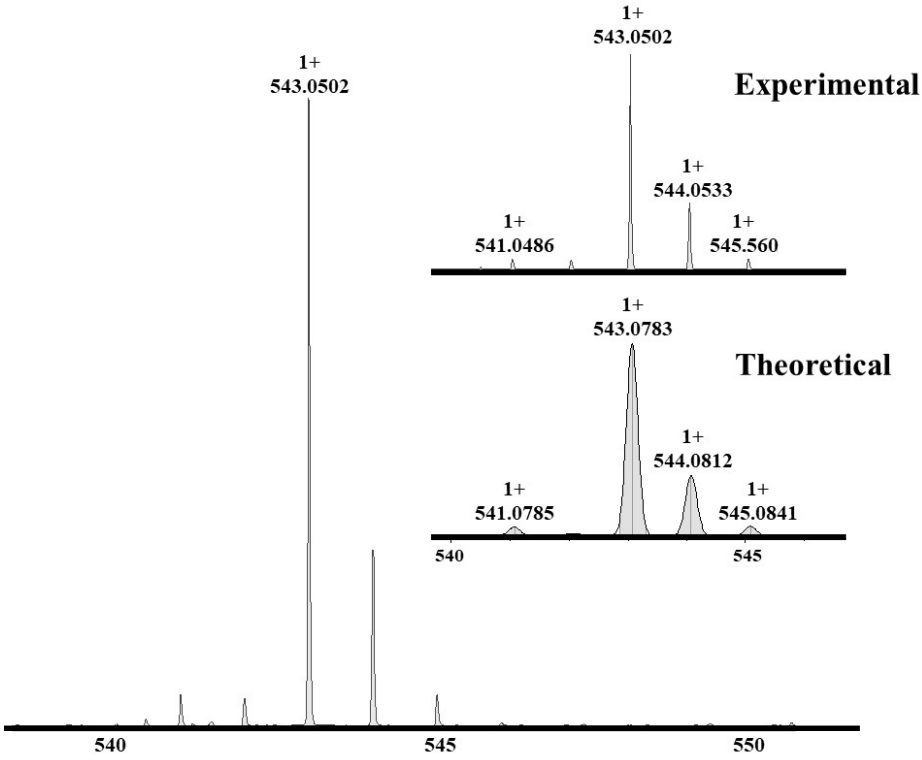

Figure S2. ESI-MS spectrum of complex **In-1** in CH_3CN. Inset: the comparison of observed and predicted isotope distribution.

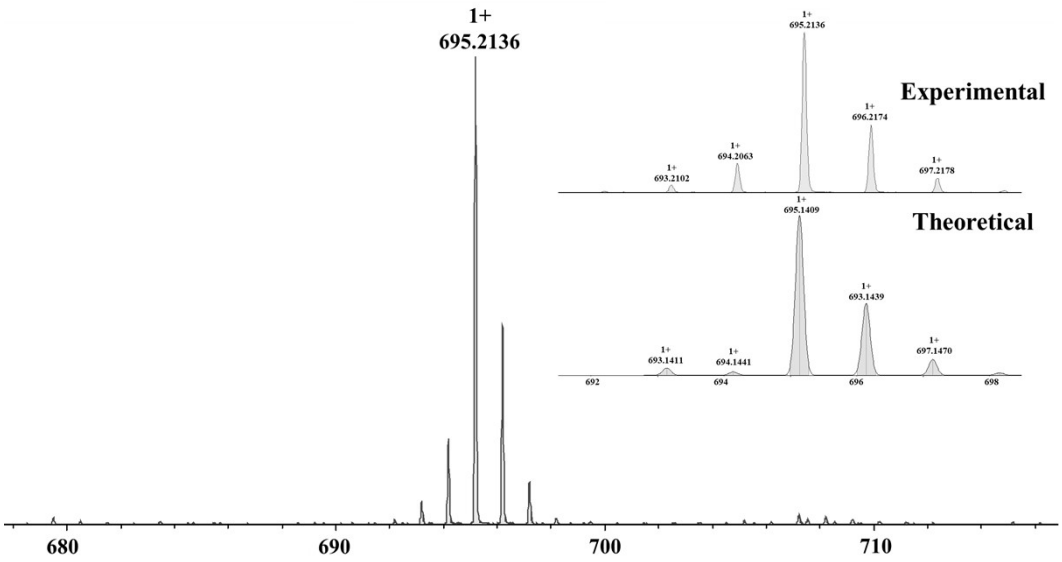

Figure S3. ESI-MS spectrum of complex **In-2** in CH_3CN. Inset: the comparison of observed and predicted isotope distribution.

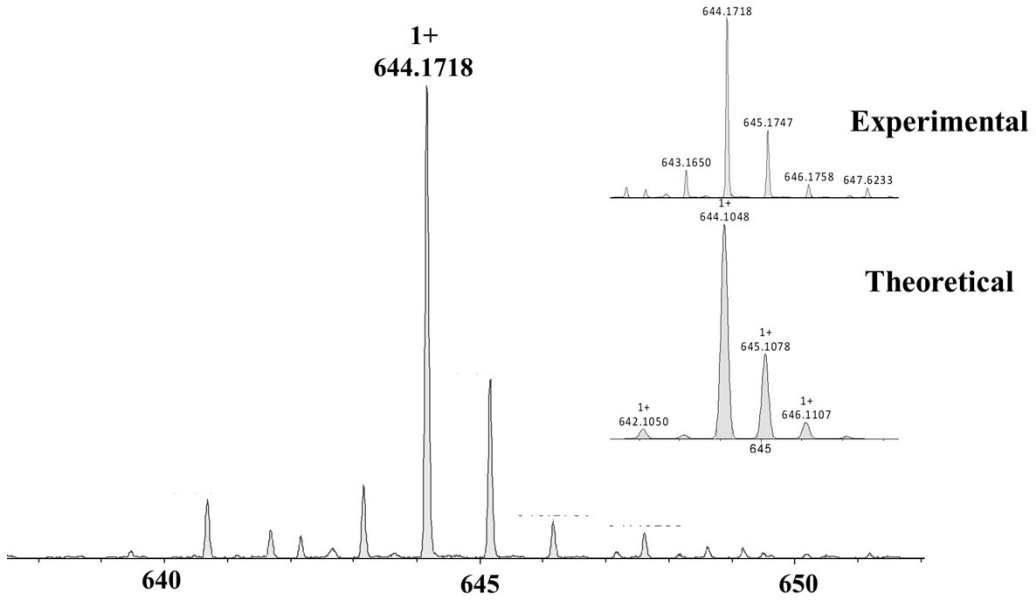

Figure S4. ESI-MS spectrum of complex **In-3** in CH_3CN. Inset: the comparison of observed and predicted isotope distribution.

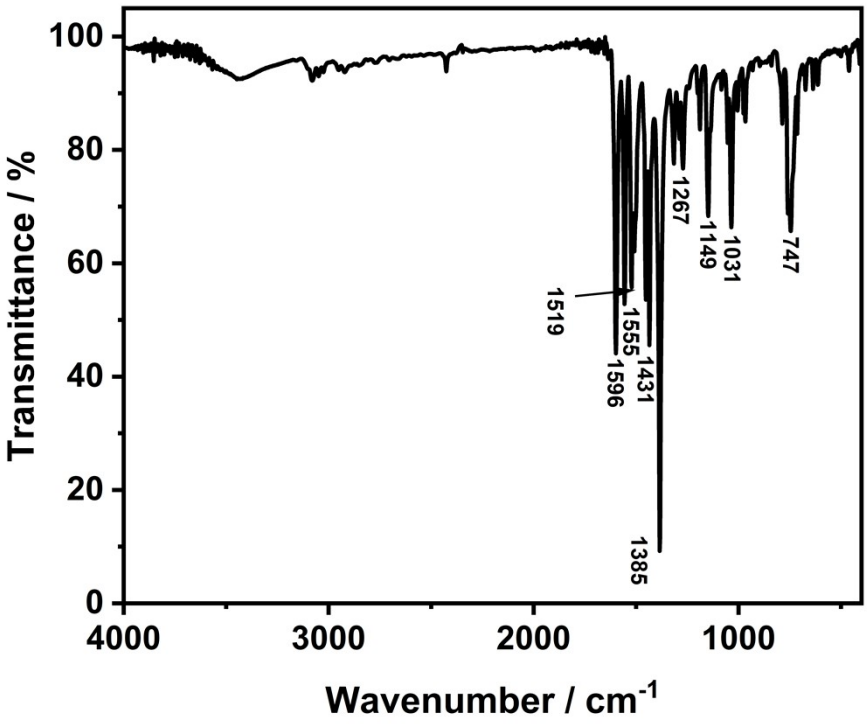

Figure S5. IR spectrum of complex **In-1**.

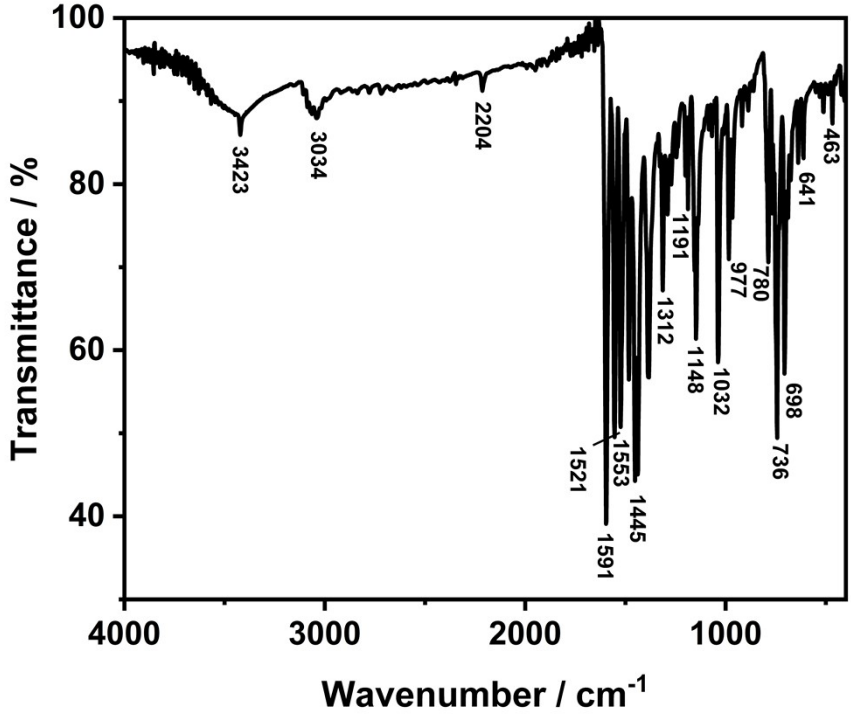

Figure S6. IR spectrum of complex **In-2**.

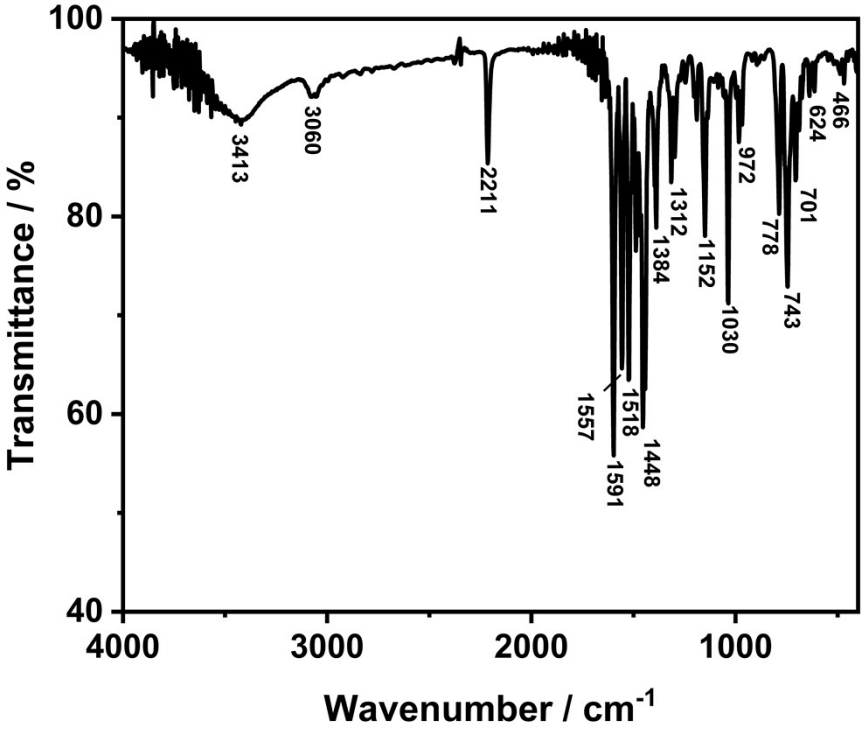

Figure S7. IR spectrum of complex **In-3**.

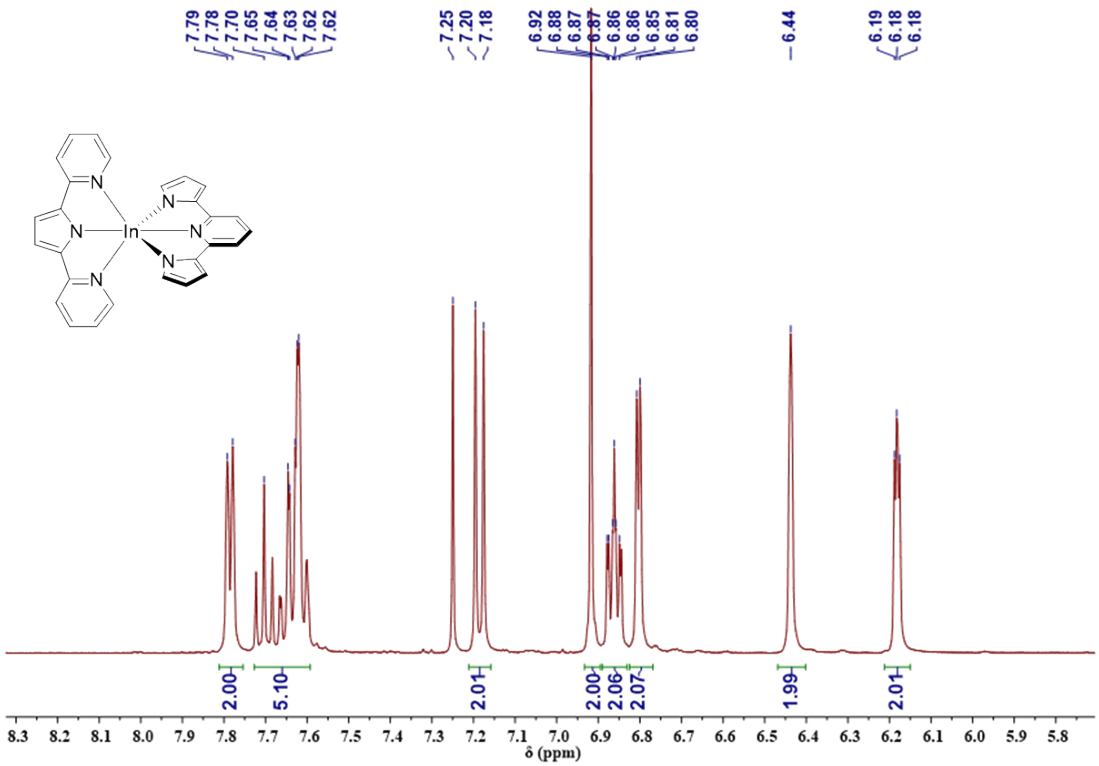

Figure S8. ^{1}H NMR spectrum of complex **In-1** in $CDCl_3$.

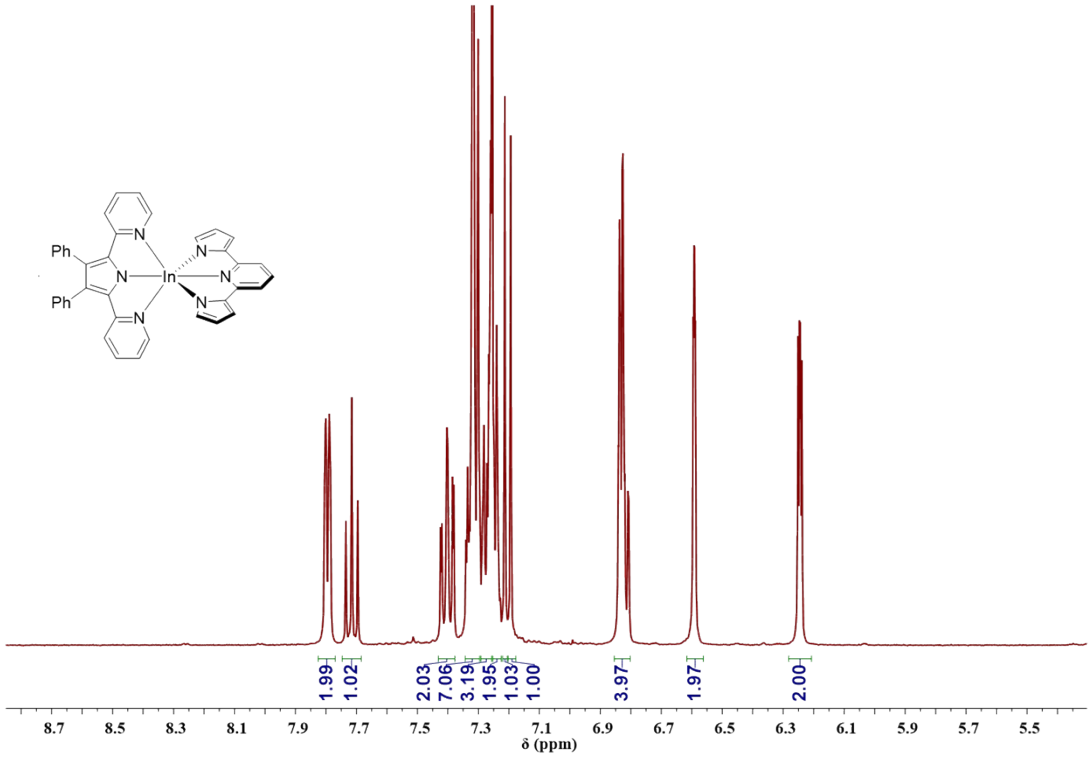

Figure S9. ^{1}H NMR spectrum of complex **In-2** in $CDCl_3$.

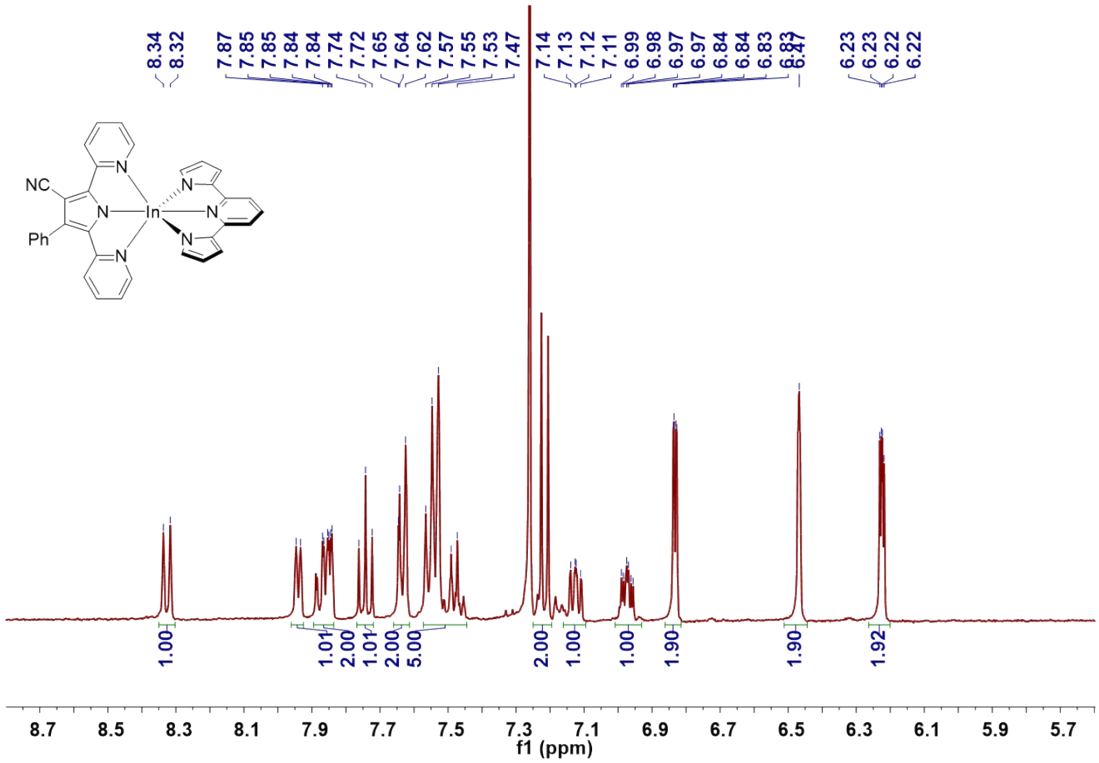

Figure S10. ^{1}H NMR spectrum of complex **In-3** in $CDCl_3$.

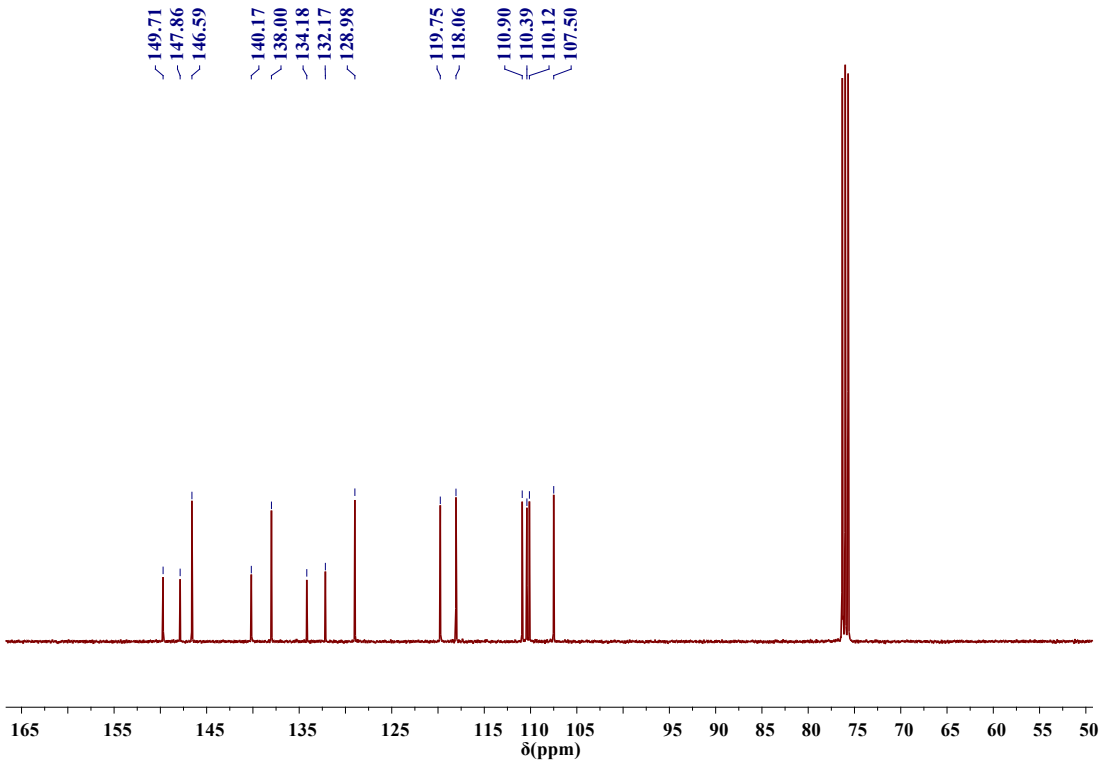

Figure S11. ^{13}C NMR spectrum of complex **In-1** in $CDCl_3$.

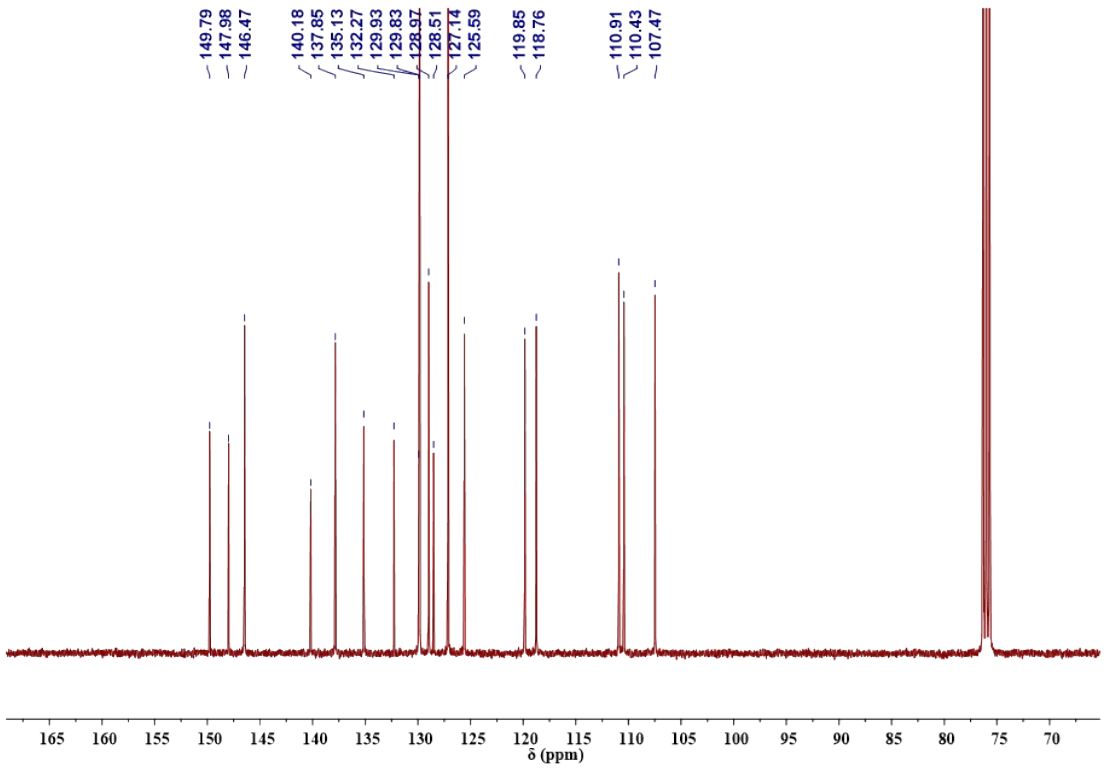

Figure S12. ^{13}C NMR spectrum of complex **In-2** in $CDCl_3$.

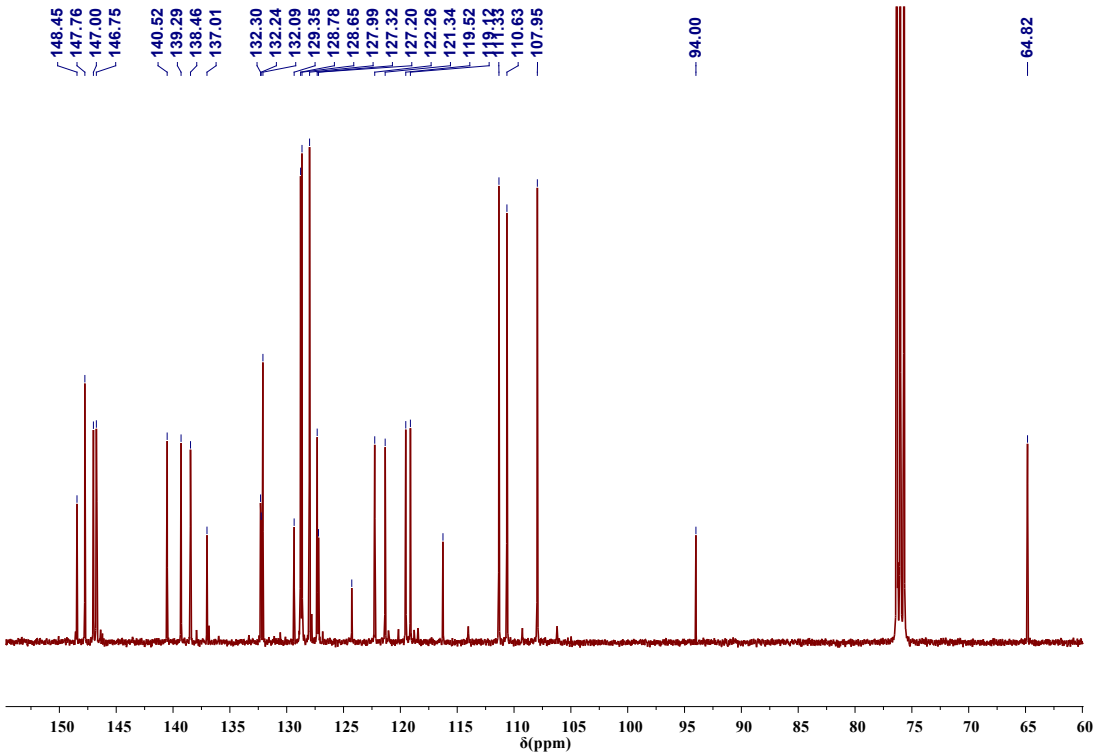

Figure S13. ^{13}C NMR spectrum of complex **In-3** in $CDCl_3$.

3. Crystallographic Data

Table S1. X-ray crystallographic data for complexes **In-1** and **In-2**.

Compound	**In-1**	**In-2**
Empirical formula	$C_{28}H_{21}Cl_2InN_6$	$C_{39}H_{27}InN_6$
Formula weight	627.23	694.48
Temperature/K	296(2)	193(2)
Crystal system	monoclinic	monoclinic
Space group (number)	$P2_1/c$ (14)	$P2_1/c$ (14)
a/Å	9.8970(6)	17.376(2)
b/Å	13.8181(9)	12.5530(14)
c/Å	19.8826(13)	15.4838(19)
α/deg	90	90
β/deg	99.115(4)	111.593(3)
γ/deg	90	90
Volume/Å^3	2684.8(3)	3140.4(6)
Z	4	4
ρ_{calc}/(g·cm^{-3})	1.552	1.469
μ/mm^{-1}	1.108	0.791
F(000)	1256	1408
Reflections collected	21703	12683
Independent reflections	5863	5437
R_{int}	0.0394	0.0755
R_{sigma}	0.0577	0.1040
Data / Restraints / Parameters	5863/820/516	5437/0/415
Goodness-of-fit on F^2	1.017	1.097
Final R indexes [$I \geq 2\sigma(I)$]	R_1 = 0.0339	R_1 = 0.0705
	wR_2 = 0.0384	wR_2 = 0.1665
Final R indexes (all data)	R_1 = 0.0827	R_1 = 0.1294
	wR_2 = 0.0429	wR_2 = 0.2103

[a] GoF = $[\Sigma w(|F_o| - |F_c|)^2/(N_{obs} - N_{param})]^{½}$.

[b] $R_1 = \Sigma||F_o| - |F_c||/\Sigma|F_o|$.

[c] wR_2 $[(\Sigma w|F_o| - |F_c|)^2/\Sigma w^2|F_o|^2]^{½}$.

Table S2. Selected bond lengths (Å) and angles (°)

Compound	**In-1**	**In-2**
	Bond lengths/Å	
In1−N1	2.225(2)	2.231(7)
In1−N2	2.158(2)	2.179(6)
In1−N3	2.168(2)	2.153(7)
In1−N4(A)	2.124(12)	2.112(6)
In1−N5(A)	2.343(15)	2.374(7)
In1−N6(A)	2.497(13)	2.396(6)
	Angle/deg	
N1−In1−N2	73.06(9)	73.2(3)
N1−In1−N3	73.26(9)	73.6(3)
N1−In1−N4(A)	171.9(4)	161.9(3)
N1−In1−N5(A)	115.1(3)	127.2(2)
N1−In1−N6(A)	104.7(3)	92.2(2)
N2−In1−N3	145.60(9)	144.3(3)
N2−In1−N4(A)	101.8(5)	105.7(2)
N2−In1−N5(A)	92.2(6)	89.2(2)
N2−In1−N6(A)	95.7(5)	101.7(2)
N3−In1−N4(A)	112.4(5)	109.9(2)
N3−In1−N5(A)	95.7(6)	100.5(3)
N3−In1−N6(A)	99.4(5)	92.4(2)
N4(A)−In1−N5(A)	70.8(4)	70.4(2)
N4(A)−In1−N6(A)	69.1(4)	70.1(2)
N5(A)−In1−N6(A)	139.9(4)	140.5(2)

4. DFT Calculation

DFT calculations were performed by using the Gaussian 09 package[3]. Geometry optimizations were performed on the ground state structures with the Becke's three-parameter B3LYP exchange-correlation functional[4,5]. The all-electron Gaussian basis sets were those developed by the Ahlrichs group[6-8]. The slightly smaller polarized split-valence def2-SVP basis sets for H, C, N and In atom Vibrational frequencies were calculated based on the optimized structures to confirm the absence of imaginary frequencies. MOs of complexes were calculated and visualized as well. The excited states calculations were carried out on the basis of the optimized S0 structures via time-dependent DFT (TD-DFT)[9] at the same level. The solvation effects were also taken into account using the self-consistent reaction field (SCRF) and a universal solvation model density (SMD)[10] with the acetonitrile solvent.

Input File Examples

Geometry Optimizations

```
%chk=In-1.chk
%mem=6GB
%nprocshared=8
#p b3lyp/def2SVP opt freq geom=connectivity

opt for In-1

0 1
Coordinates
```

TD-DFT Calculations

```
%chk=In-1-uv.chk
%mem=6GB
%nprocshared=8
#p td=(50-50, nstates=50, root=1) b3lyp/def2SVP SCRF(SMD,solvent=acetonitrile) geom=connectivity

uv for In-1

0 1
Coordinates
```

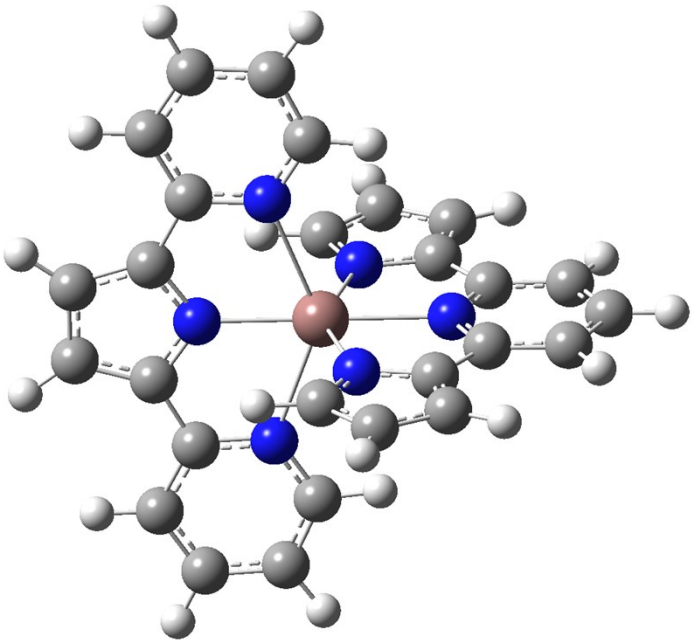

Figure S14. Optimized geometries for **In-1**

Table S3 Comparison of selected bond lengths (Å) of **In-1** from experimental and calculated results

Bond length/angle	Calc. (In-1)	Exp. (In-1)
In-N1	2.20951	2.225(2)
In-N2	2.26548	2.168(2)
In-N3	2.20955	2.158(2)
In-N4	2.48370	2.343(15)
In-N5	2.14041	2.124(12)
In-N6	2.48390	2.497(13)

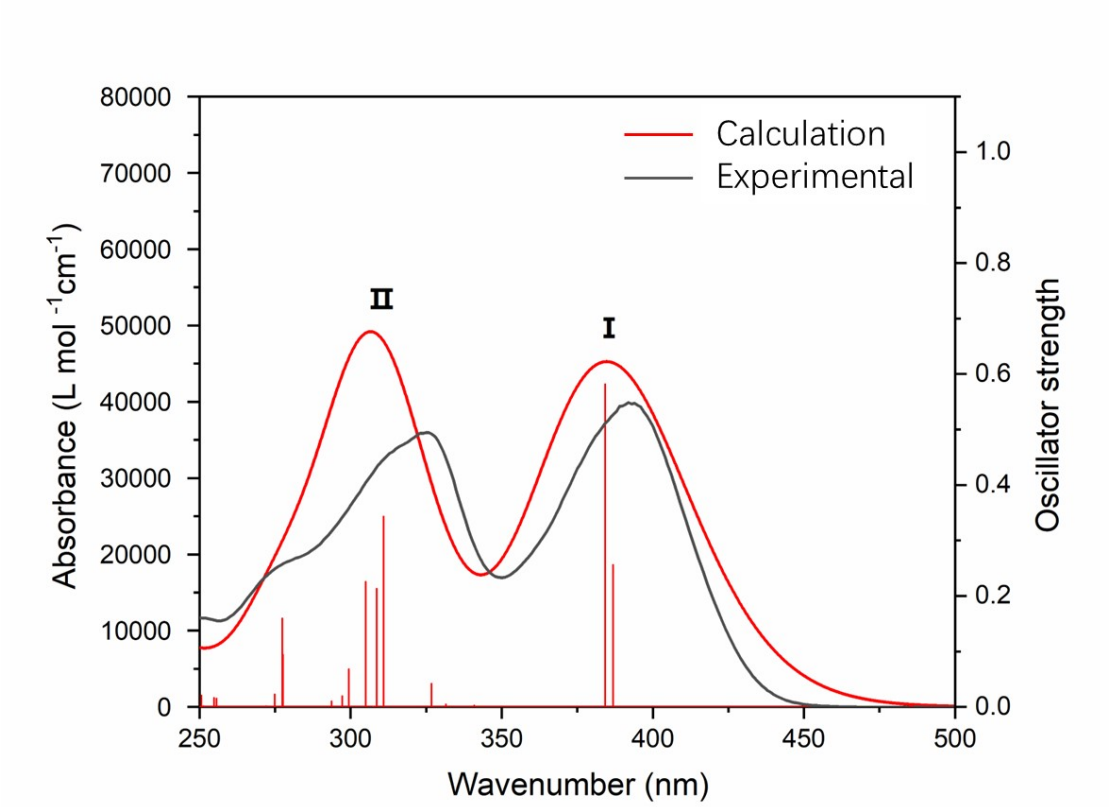

Figure S15. Electronic absorption spectrum of **In-1** obtained via TD-DFT calculations (red line, fwhm of 0.5 eV). The stick plot indicates the positions and relative intensities of individual transitions. Transitions with calculated oscillator strengths larger than 0.03 are labeled according to their TD-DFT state number. The experimental spectrum is shown as a grey line for comparison.

Table S4 Vertical Electronic Excitation Energies and Main Excitations Contributing to the Absorption Bands of **In-1** Obtained via TD-DFT Calculations.

	band	state	E (eV)	λ (nm)	f_{osc}	Excitations (weight)[a,b]	Character
In-1	**I**	6	3.2056	386.77	0.2563	122→124 (0.98)	^{1}ILCT
		7	3.2268	384.24	0.5815	121→123 (0.98)	^{1}ILCT
	II	21	3.7947	326.73	0.0419	121→125 (0.92)	^{1}IL + ^{1}LLCT
		26	3.9884	310.86	0.3431	122→126 (0.64)	^{1}IL + ^{1}LLCT
						120→124 (0.25)	^{1}IL
						118→124 (0.05)	^{1}IL
		27	4.0175	308.61	0.2131	121→127 (0.96)	^{1}IL
		30	4.0653	304.98	0.2253	120→125 (0.56)	^{1}IL + ^{1}LLCT
						120→126 (0.39)	^{1}IL + ^{1}LLCT
		34	4.1411	299.40	0.0681	120→125 (0.43)	^{1}IL + ^{1}LLCT
						120→126 (0.55)	^{1}IL + ^{1}LLCT
		37	4.1707	297.27	0.0193	119→123 (0.49)	^{1}LLCT
		39	4.2208	293.75	0.0099	117→123 (0.29)	^{1}IL
						121→128 (0.38)	^{1}IL
		44	4.4657	277.63	0.0941	117→123 (0.20)	^{1}IL
						121→128 (0.54)	^{1}IL
		45	4.4696	277.40	0.1593	119→124 (0.93)	^{1}IL
						120→126 (0.05)	^{1}IL + ^{1}LLCT
		46	4.5102	274.89	0.0226	118→124 (0.91)	^{1}IL

[a] Only excitations contribution with a weight larger than 0.05 are shown. [b] for **In-1**: HOMO 122, LUMO 123.

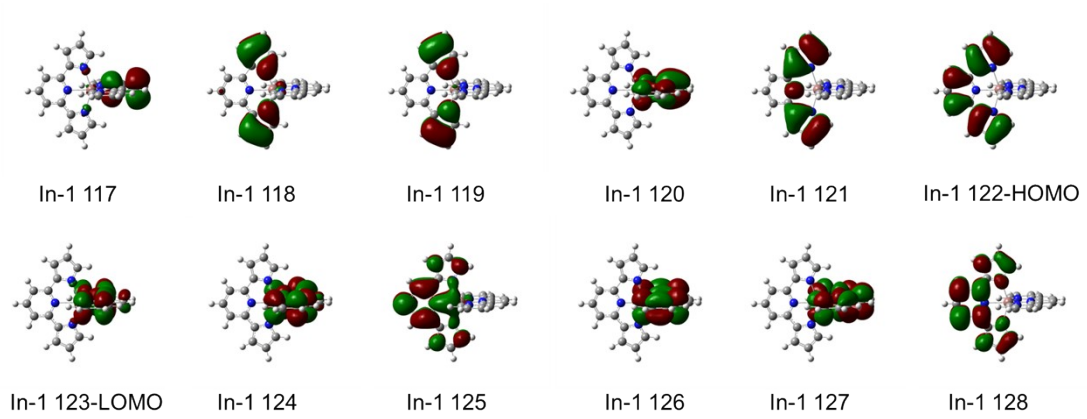

Figure S16. Frontier molecular orbital diagram of **In-1** showing the donor and acceptor orbitals contributing to TD-DFT excitations computed in visible region of electronic absorption spectrum.

5. Lifetime, absorption and Emission Spectra in Various Solvents

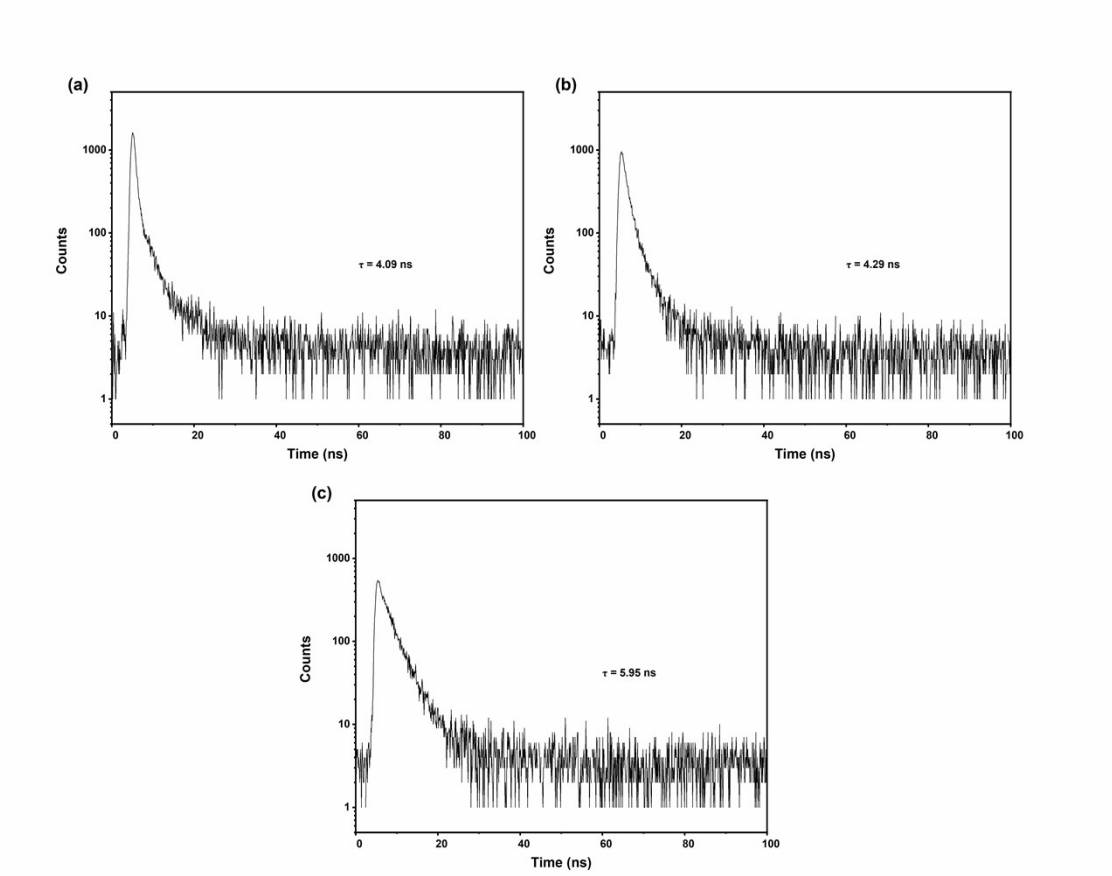

Fig. S17. Exited-state lifetime measurements of **In-1** (a), **In-2** (b) and **In-3** (c) under argon atmosphere.

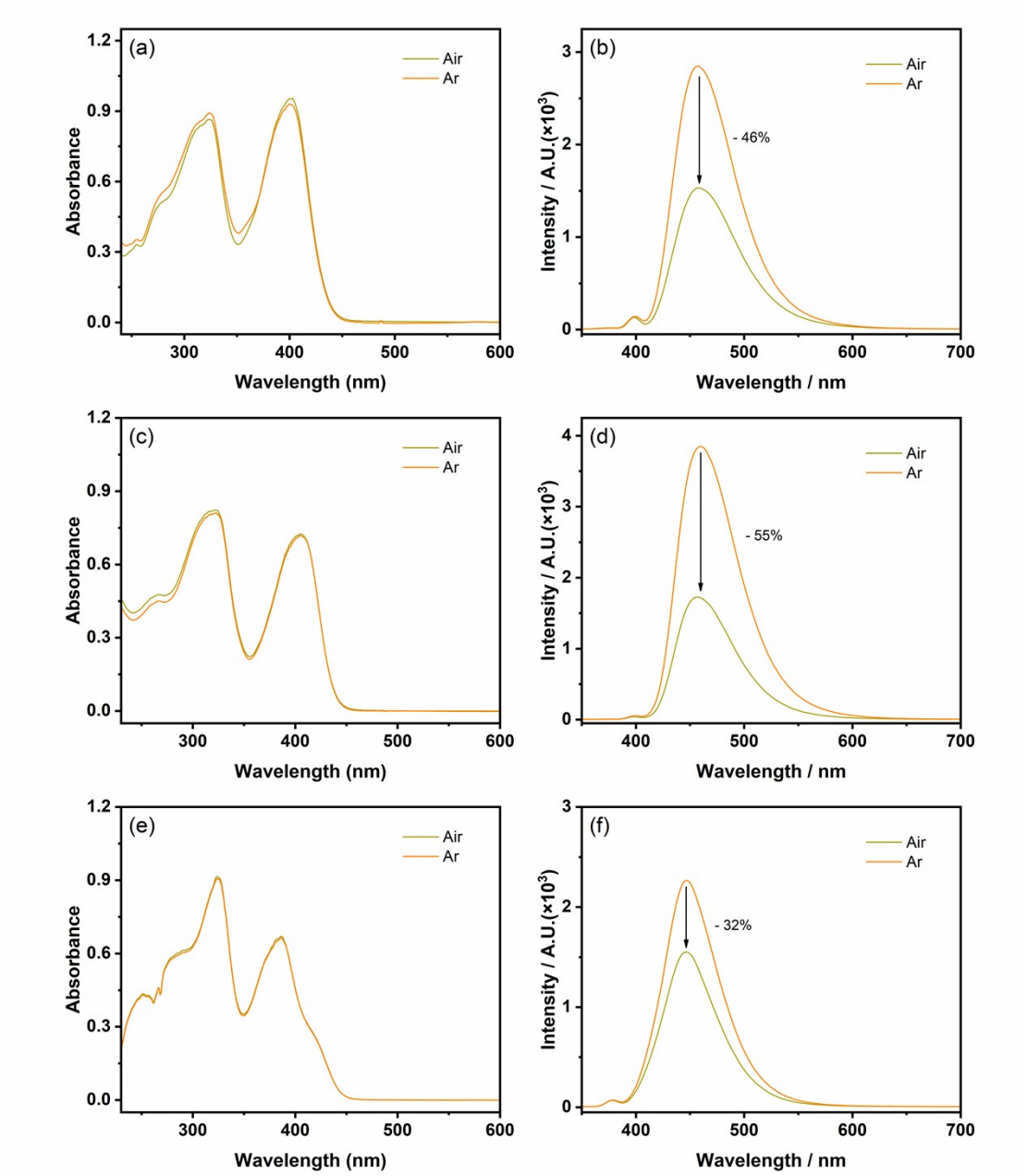

Figure S18. The absorption spectra (a) and emission spectra (b) of **In-1** in CH_3CN solution under argon atmosphere or upon exposure to air; The absorption spectra (c) and emission spectra (d) of **In-2** in CH_3CN solution under argon atmosphere or upon exposure to air; The absorption spectra (e) and emission spectra (f) of **In-3** in CH_3CN solution under argon atmosphere or upon exposure to air.

6. Photoredox Catalysis

7.1 Experimental setup for CO_2 reduction

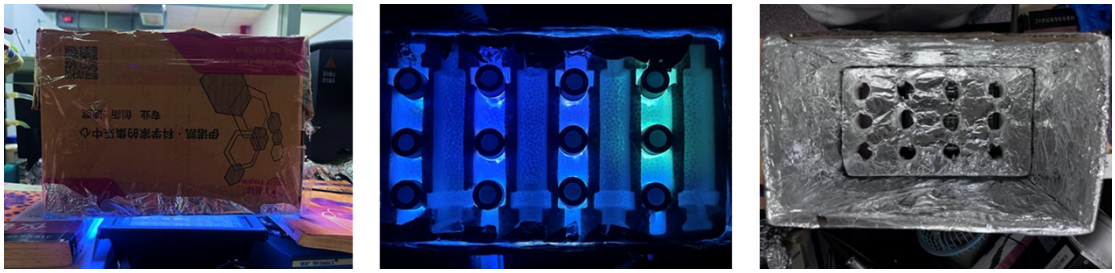

Figure S19. Experimental setup for irradiation.

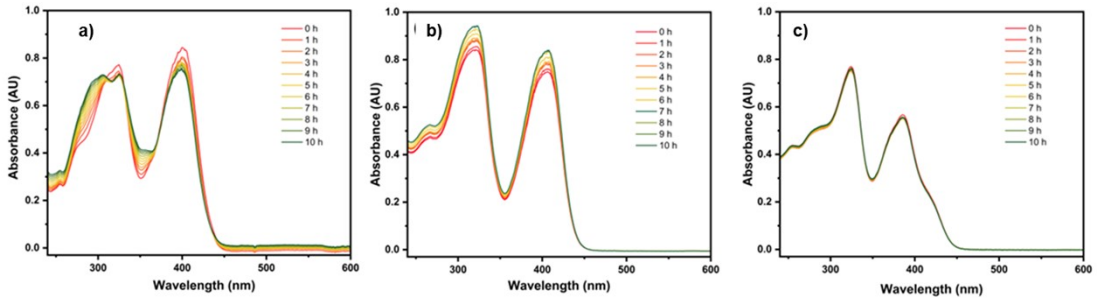

Figure S20. Stability monitored by UV-vis spectroscopy. UV-vis spectra of 50 μM (a) **In-1**, (b) **In-2** and (c) **In-3** in 0.3 M TEOA CH_3CN solutions within 10 h, indicating that Al-1 is less stable than other methylated analogues in the reaction media

Table S5. Photocatalytic CO_2 reduction to CO in the absence of certain component*

Entry	Conditions	n(CO) (μmol)	n(H_2) (μmol)
1	No catalyst	N.D.	trace
2	Under N_2 instead of CO_2	N.D.	trace
3	No PS	N.D.	N.D.
4	No BIH	N.D.	trace

*Standard condition： **In-1** (0.5 mM), CoPc (0.05 mM), BIH (50 mM) and TEOA (0.3 M) in 5 mL CH_3CN within 6 h of 365-nm LED irradiation under 1 atm CO_2.

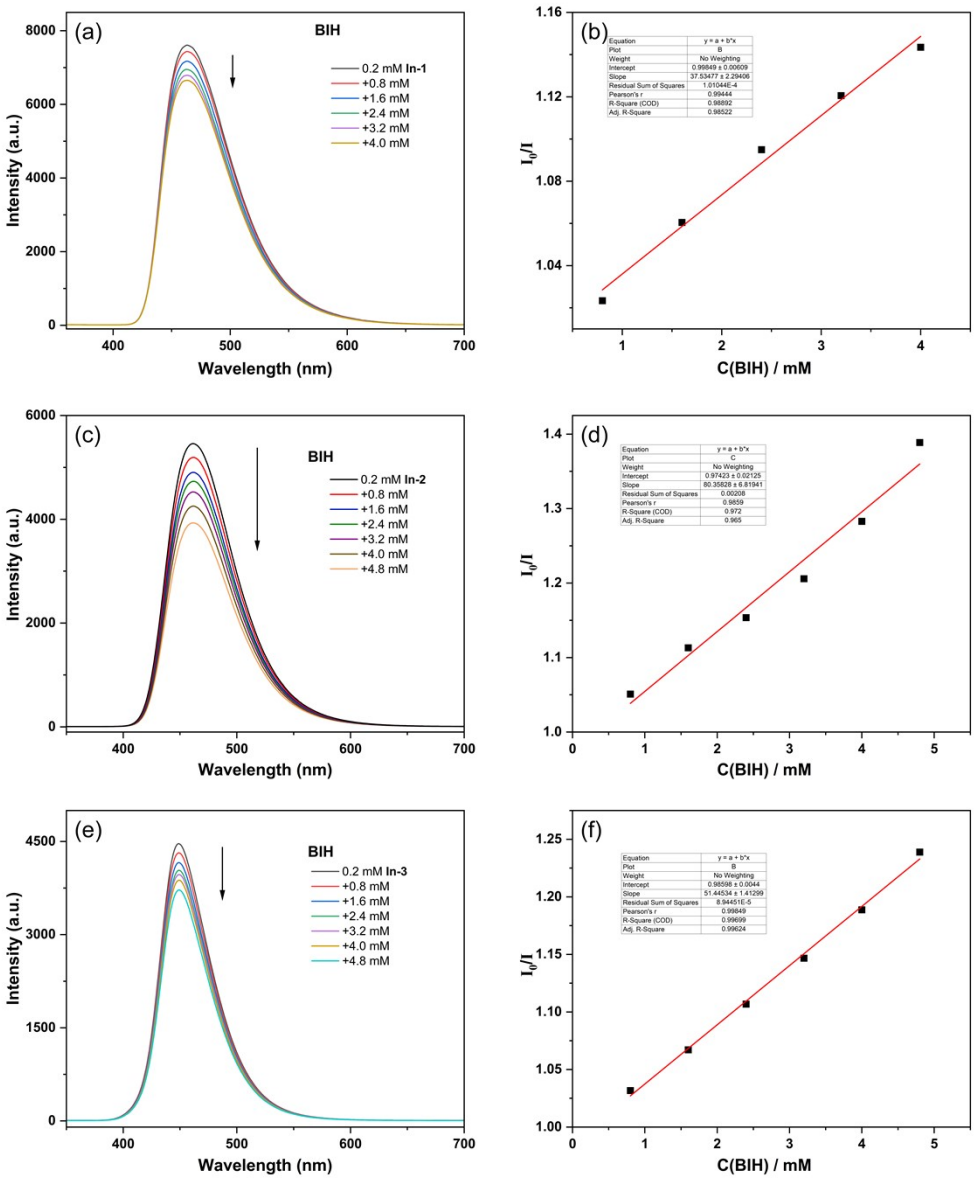

Figure S21. The fluorescence quenching curves of (a) **In-1**, (c) **In-2,** (e) **In-3** with BIH. (b)(d)(e) BIH on **In-1, In-2** and **In-3** Stern-Volmer quenching curve. K_q(**In-1**)=9.17×10^9 $M^{-1}S^{-1}$;K_q(**In-2**)=1.87×10^9 $M^{-1}S^{-1}$; K_q(**In-3**)=8.57×10^9 $M^{-1}S^{-1}$

7. References

1. McPherson, J. N.; Das, B.; Colbran, S. B. *Coord. Chem. Rev.* **2018**, *375*, 285-332.
2. McSkimming, A.; Diachenko, V.; London, R.; Olrich, K.; Onie, C. J.; Bhadbhade, M. M.; Bucknall, M. P.; Read, R. W.; Colbran, S. B. *Chem. Eur. J.* **2014**, *20*, 11445-11456.
3. Frisch, M. J., Trucks, G. W., Schlegel, H. B., Scuseria, G. E., Robb, M. A., Cheeseman, J. R., Scalmani, G., Barone, V., Mennucci, B., Petersson, G. A., Nakatsuji, H., Caricato, M., Li, X., Hratchian, H. P., Izmaylov, A. F., Bloino, J., Zheng, G., Sonnenberg, J. L., Hada, M., Ehara, M., Toyota, K., Fukuda, R., Hasegawa, J., Ishida, M., Nakajima, T., Honda, Y., Kitao, O., Nakai, H., Vreven, T., Montgomery, J. A., Jr., Peralta, J. E., Ogliaro, F., Bearpark, M., Heyd, J. J., Brothers, E., Kudin, K. N., Staroverov, V. N., Keith, T., Kobayashi, R., Normand, J., Raghavachari, K., Rendell, A., Burant, J. C., Iyengar, S. S., Tomasi, J., Cossi, M., Rega, N., Millam, N. J., Klene, M., Knox, J. E., Cross, J. B., Bakken, V., Adamo, C., Jaramillo, J., Gomperts, R., Stratmann, R. E., Yazyev, O., Austin, A. J., Cammi, R., Pomelli, C., Ochterski, J. W., Martin, R. L., Morokuma, K., Zakrzewski, V. G., Voth, G. A., Salvador, P., Dannenberg, J. J., Dapprich, S., Daniels, A. D., Farkas, O., Foresman, J. B., Ortiz, J. V., Cioslowski, J. & Fox, D. J. *Gaussian 09, Revision D.01*; Gaussian, Inc.: Wallingford CT, 2009.
4. Becke, A. D., *J. Chem. Phys.,* **1993**, 98, 5648-5652.
5. Lee, C., Yang, W. and Parr, R. G., *Phys. Rev. B,* **1988**, 37, 785-789.
6. Schäfer, A., Horn, H. and Ahlrichs, R., *J. Chem. Phys.,* **1992**, 97, 2571.
7. Schäfer, A., Huber, C. and Ahlrichs, R., *J. Chem. Phys.,* **1994**, 100, 5829.
8. Weigend. F. and Ahlrichs R., *Phys. Chem. Chem. Phys.,* **2005**, 7, 3297.
9. Fantacci, S., De Angelis, F. and Selloni, A., *J. Am. Chem. Soc.,* **2003**, 125, 4381-4387.
10. Marenich A. V., Cramer C. J., and Truhlar D. G. *J. Phys. Chem. B,* **2009**, 113, 6378-6396.